Journal of Inorganic Biochemistry 199 (2019) 110787

Contents lists available at ScienceDirect

Journal of Inorganic Biochemistry

journal homepage: www.elsevier.com/locate/jinorgbio

A new amido-phosphine of dichloroacetic acid as an active ligand for metals of pharmaceutical interest. Synthesis, characterization and tests of antiproliferative and pro-apoptotic activity

Lorenza Marvelli[a], Valeria Ferretti[a], Valerio Bertolasi[a], Ilaria Lampronti[b], Roberto Gambari[b], Claudio Trapella[a], Giulia Turrin[a], Francesca Bonotto[a], Antonio Moriello[a], Paola Bergamini[a,*]

[a] Dipartimento di Scienze Chimiche e Farmaceutiche, Università degli Studi di Ferrara, via L. Borsari 46, 44121 Ferrara, Italy
[b] Dipartimento di Scienze della Vita e Biotecnologie, Sezione di Biochimica e Biologia Molecolare, Università degli Studi di Ferrara, via Fossato di Mortara 74, 44121 Ferrara, Italy

ARTICLE INFO

Keywords:
Inorganic drugs
Anticancer complexes
Dichloroacetic acid
Cell apoptosis
Antiproliferative activity

ABSTRACT

We herein describe the synthesis and characterization of the new amido-phosphinic ligand 3,7-bis(dichloroacetyl)-1,3,7-triaza-5-phosphabicyclo[3.3.1]nonane (DCP), a derivative of dichloroacetic acid (DCA), whose ability to reverse the suppressed mitochondrial apoptosis in cancer cells is known. DCP was obtained by a double N-acylation of PTA (1,3,5-triaza-7-phosphaadamantane) occurring with loss of CH_2, in appropriate conditions. Due to the hindered rotation around the amidic CN bonds, three rotameric forms of DCP were observed, whose ratio in solution was dependent on the solvent, while the X-ray crystal structure of DCP showed an opposite orientation of the two amidic carbonyl groups (*anti* rotamer). The lipophilic, air and thermally stable DCP was found able to act regiospecifically as a P-donor ligand toward soft metal ions. By ligand substitution on appropriate precursors, we obtained the complexes **1–9**, where proapoptotic DCA is associated with metal ions of known cytotoxic activity on cancer cells (Pt^{2+}, Pd^{2+}, Ru^{2+}, Re^{+}, Au^{+}). The antiproliferative activity of DCP and its complexes was tested in vitro, in comparison with cisplatin, on three human tumor cell lines: A2780 (ovarian cisplatin-sensitive), A2780*cis* (ovarian cisplatin-resistant) and K562 (erythroleukemic). The results showed that the simultaneous presence of DCP (containing two residues of proapoptotic DCA) and Pt(II) produces the best performances with respect to non-platinum complexes. Experiments of pro-apoptotic activity indicated that the antiproliferative activity of the most active DCP-Pt(II) complexes is associated with induction of apoptosis.

1. Introduction

The aliphatic phosphine PTA (1,3,5-triaza-7-phosphaadamantane) is a stable water soluble ligand widely used in metal complexes for many purposes, including catalysis [1–5], new materials [6–8], and metal-based therapeutics [9–12]. The basic structure can be modified at each position under appropriate conditions. We [13–17] and others [18–21] described several N-alkylation reactions, which occurred with complete regioselectivity on a single nitrogen producing cationic derivatives still able to give metal coordination through phosphorus donor (Fig. 1a). In 2004 and in 2007, two examples of PTA derivatives obtained by N-acylation were reported: 3,7-diacetyl-1,3,7-triaza-5-phosphabicyclo[3.3.1]nonane (DAPTA) and 3,7-diformyl-1,3,7-triaza-5-phosphabicyclo[3.3.1]nonane (DFPTA) (Fig. 1b) [22–23].

While the N-alkylation of PTA generates quaternary ammonium cations, the acylation involves two nitrogen atoms, with loss of a CH_2 bridge, producing neutral structures where the adamantane-like cage is open.

Inspired by these molecules, DAPTA and DFPTA, due to our interest in metal-based drugs, we designed the analogue 3,7-bis(dichloroacetyl)-1,3,7-triaza-5-phosphabicyclo[3.3.1]nonane (DCP), where PTA is functionalized with dichloroacetyl groups, (Fig. 2).

Dichloroacetic acid (DCA) is an orphan drug used for lactic acidosis, but recently it has attracted attention also as potential anticancer because of its ability to interfere selectively with the mechanism that makes cancer cells resistant to normal apoptotic processes. Several reports demonstrated that the DCA antitumor activity (also overcoming resistance to usual chemotherapy) is related to its ability to re-activate mitochondrial metabolism in tumor cells [24–25]. Nevertheless, its application is limited by the high concentrations needed for significant

* Corresponding author.
E-mail address: bgp@unife.it (P. Bergamini).

https://doi.org/10.1016/j.jinorgbio.2019.110787
Received 3 April 2019; Received in revised form 18 July 2019; Accepted 19 July 2019
Available online 22 July 2019

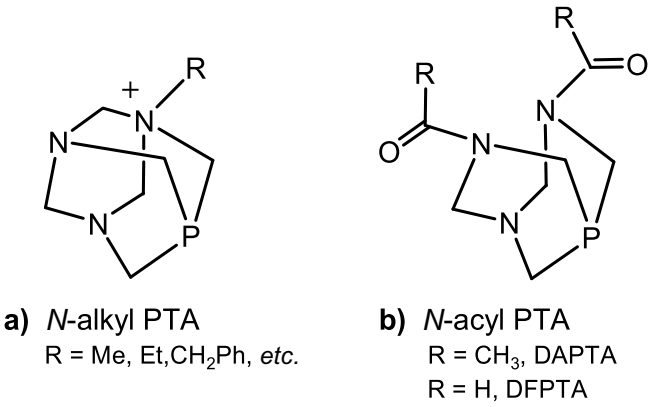

Fig. 1. General structures of *N*-alkyl PTA (**a**) and *N*-acyl PTA (**b**).

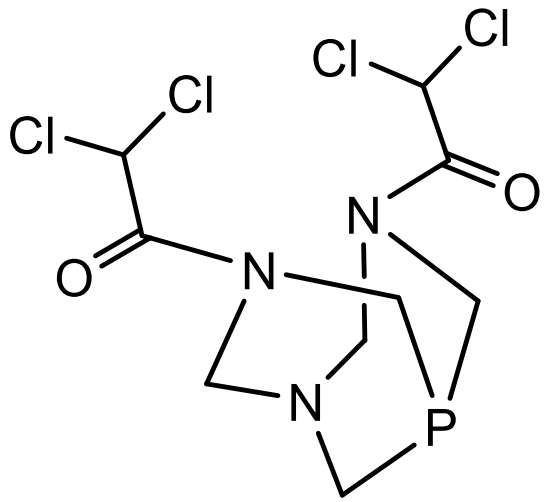

Fig. 2. DCP, 3,7-bis(dichloroacetyl)-1,3,7-triaza-5 phosphabicyclo[3.3.1] nonane.

therapeutic effect, producing detrimental side effects involving the nervous system [26]. For this reason there is a great interest in the development of DCA derivatives hopefully provided with a better therapeutic index. This aim has been previously pursued introducing DCA in large lipophilic molecules as an ester [27] or an amide [28].

In this work we propose the design and development of the new phosphino-amide DCP, potentially able to behave both as lipophilic carrier of DCA and as ligand for metal ions. DCP is the first reported example of phosphinic derivative of dichloroacetic acid. The chemical aims of the present work are to optimize its synthesis, to characterize it both in solution and in the solid state and to screen its ability to act as a ligand for a variety of metal ions. The metal complexes of DCP, combining dichloroacetic acid and an active metal ion (e.g. Pt^{2+}, Pd^{2+}, Ru^{2+}) in the same molecule, could act as anticancer drugs provided of dual therapeutic action, pro-apoptotic (mitochondria reactivator) and antiproliferative (DNA or essential proteins damaging agents) toward cancer cells. A series of biochemical experiments have been conducted in order to see if the presence of a dichloroacetic derivative boosts the effect of metal complexes.

2. Results and discussion

2.1. Synthesis and characterization of 3,7-bis (dichloroacetyl)-1,3,7-triaza-5-phosphabicyclo[3.3.1]nonane (DCP)

The reported N-acyl derivatives of PTA, DAPTA [22] and DFPTA [23], were obtained by treating PTA with an excess of acetyl anhydride and formyl anhydride respectively, in water. Following the same procedure with DCA anhydride, only PTA was recovered in its N-protonated form, as shown by the small shift in the ^{31}P signal (from −98 ppm of PTA to −91 ppm of $PTAH^+$) [29]. In fact the formation of DCP implies the releasing of two equivalents of dichloroacetic acid (Scheme 1), a much stronger acid than acetic and formic acid, released in the formation of DAPTA e DFPTA respectively. DCA is able to protonate PTA, reducing its nucleophilic power and therefore inhibiting its reaction with the anhydride.

We found that the basicity of the reaction medium is the crucial parameter in the synthesis of DCP. The yield increased from *ca* 10% obtained using $NaHCO_3$ (pH 8.35) to *ca* 74.5% with Na_2CO_3 (0.12 M, pH 11.7). The volume of the basic solution was modulated to have Na_2CO_3 in molar excess with respect to the DCA anhydride. In fact the chloroacetic acid, progressively formed by the reaction, reacts with part of sodium carbonate giving a $NaHCO_3/Na_2CO_3$ buffer solution (measured pH = 9.3), which prevents the protonation of PTA.

The new amido-phosphine DCP was characterized by several techniques. In HPLC-ESI MS, DCP presents a single peak at 368 (M + 1), but the NMR investigation in DMSO shows the presence of three rotamers due to the double bond character of the amidic N═C−O group (Fig. 3) [30].

Also for DAPTA [31] and DFPTA [23] several species were observed by NMR, whose number was depending on the solvent.

In the case of DCP, in DMSO, the ^{31}P NMR showed three single signals at δ −78.5, −68.8 e –68.4 ppm in a 1:7:1 estimated intensity ratio. The ^1H NMR spectrum in DMSO-d_6 showed four singlets for the $COCHCl_2$ group of DCA at 7.07, 7.18, 7.20 and 7.28 ppm, with an intensity ratio of 1:1:4:4, exactly reproducible in different preparations. We assigned the pair of intense signals at 7.20 and 7.28 ppm to the two nonequivalent $COCHCl_2$ groups of the *anti* rotamer. The 1:1:8 ratio was in fair agreement with that observed in ^{31}P NMR (1:1:7).

Trying to see if the rotational barrier could be overtaken, we tried high temperature NMR experiments in DMSO-d_6. In ^{31}P NMR, one signal was observed at 120 °C, but its accentuate broadening did not allow to conclude if it was effectively a single peak or if it contained other signals in its width [32].

In acetone, DCP is present as a single rotamer (*anti*). In ^{31}P NMR, a single peak was found at −69.2 ppm and the ^1H NMR spectrum showed two equally intense singlets, due to the inequivalent $CHCl_2$ groups of the *anti* rotamer at 6.82 and 6.90 ppm. Nine signals due to the ten cage protons were also observed between 3.5 and 5.7 ppm. We assigned them on the basis of a COSY experiment. In Table 1 the ^1H NMR data in acetone of the ten cage protons of DCP and their attributions are compared with the corresponding reported for DAPTA by Laguna et al. [31].

All the geminal diastereotopic protons of CH_2 (except Hc) gave distinct signals. This observation supports the identification of DCP in acetone as the *anti* rotamer, the only one where the P atom is a stereogenic center because the two N═$COCHCl_2$ groups have different geometries (Z and E) [33].

Concerning the solid state, DCP was re-crystallized by slow cooling of an acetone solution taken to 45 °C and the X-ray crystal structure was acquired.

The crystal structure of DCP confirms that the molecule is present as the *anti* rotamer, in view of the relative position of the $CHCl_2C$═O groups (Fig. 4). The C1 atom lies on the crystallographic twofold rotation axis, so that P1 and N1 atoms are interchangeable; the disorder has been modelled refining the two atoms on the same position and giving them a 50% occupancy. As a consequence, C1-P1/N1 distances have high estimated standard deviations and are respectively shorter/longer than the standard ones (Tables 2 and 3).

Although DCP and DAPTA have a similar structure, their solubility in water is remarkably different. The presence of four bulky hydrophobic chlorine atoms enormously decreases the solubility in water (S_M of DCP < 2.7 μM) with respect to the non-chlorinated analogue

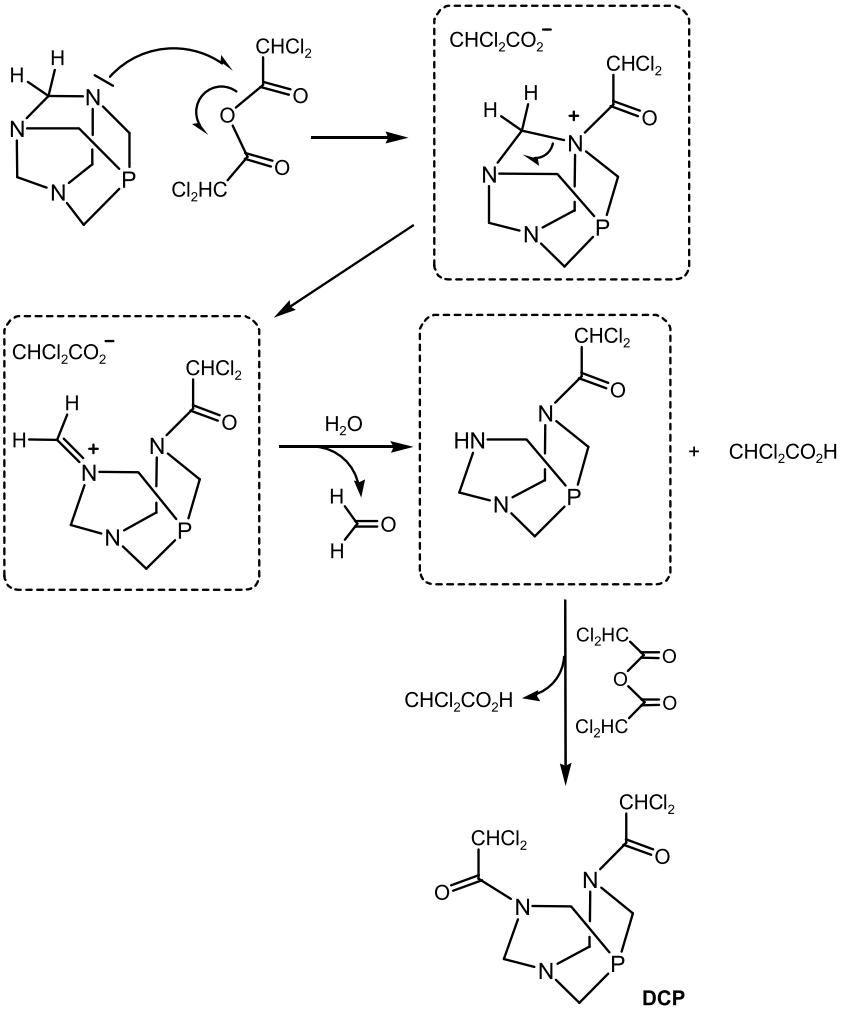

Scheme 1. Synthesis of 3,7-bis(dichloroacetyl)-1,3,7-triaza-5-phosphabicyclo[3.3.1]nonane (DCP).

DAPTA, reported as the most water soluble phosphine (S_M = 7.4 M) [22]. DCP is soluble in a 10:1 DMSO/H_2O mixture ($S_M = 2.5 \cdot 10^{-2}$ M), where is stable for at least 10 days at ^{31}P NMR observation, and also in DMF, in acetone and in CH_3CN.

2.2. Coordination of 3,7-bis(dichloroacetyl)-1,3,7-triaza-5-phosphabicyclo [3.3.1]nonane (DCP) to metal ions

The acylation of PTA involves two nitrogen atoms, leaving the phosphorus atom available for coordination to metals, including Pt^{2+}, Pd^{2+}, Ru^{2+}, Re^{+} and Au^{+} which are exploited or under investigation for their anticancer activity.

We realized the coordination of DCP to these metals, obtaining products **1**–**9**, where the new ligand is introduced following the pattern of complexes whose cytotoxic activity has been reported.

2.2.1. Pt(II) complexes of DCP: synthesis and characterization

We prepared a series of Pt(II) complexes (**1**–**4**) of the new ligand DCP, bearing an increasing number of DCA residues (Fig. 5).

Following the classical scheme of Pt anticancer drugs, two neutral ligands, two anionic ligands, *cis* disposition, we designed *cis*-[$PtCl_2$(DCP)$_2$] (**2**), which was obtained in good yield (79%) through the direct reaction of DCP with commercial K_2PtCl_4 (2:1 ratio) in CH_3CN.

The ^{31}P NMR spectrum of *cis*-[$PtCl_2$(DCP)$_2$] appeared different in different solvents: in acetone it showed two singlets with satellites at −27.3 ($^1J_{PtP}$ = 3389 Hz) and −27.1 ($^1J_{PtP}$ = 3341 Hz) which we attributed to the two diastereomeric forms (*meso* and racemate), due to

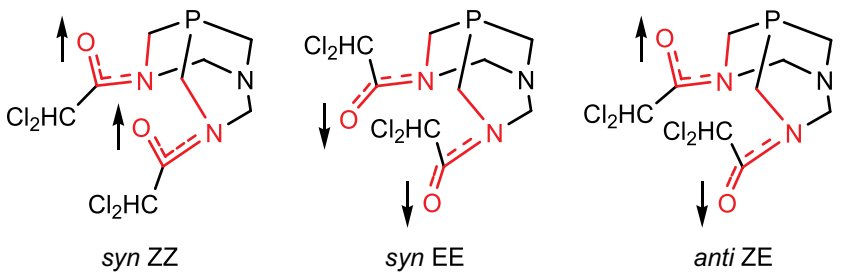

Fig. 3. Three rotameric forms of DCP. (For interpretation of the references to color in this figure, the reader is referred to the web version of this article.)

Table 1
^{1}H NMR data in acetone and attributions of the ten cage protons of DCP and DAPTA.

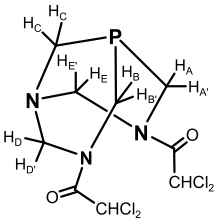

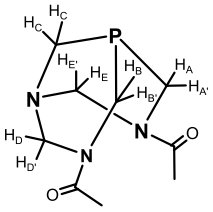

	DCP Acetone-d_6, δ (ppm); J(Hz)	DAPTA $CDCl_3$, δ (ppm); J(Hz), [31]
H_A	3.60 dt, $^2J_{HH}$ = $^2J_{PH}$ 15.1, $^2J_{HH}$ 2.3	3.20 dt, $^2J_{HH}$ = $^2J_{PH}$ 15.2, $^4J_{HH}$ 2.5
H_C	3.78 d, $^2J_{PH}$ 11.3	3.51 d, $^2J_{PH}$ 11.4
H_B	4.15 dt, $^2J_{HH}$ = $^2J_{PH}$ 14.7, $^4J_{HH}$ 2.3	3.79 ddd, $^2J_{HH}$ 15.4, $^2J_{PH}$ 4.7, $^4J_{HH}$ 2.8
H_D	4.32 d, $^2J_{HH}$ 13.7	3.95 d, $^2J_{HH}$ 14.0
H_B	4.63 d, $^2J_{HH}$ 15.0	4.28 d, $^2J_{HH}$ 15.4
H_E	4.78 d, $^2J_{HH}$ 13.9	4.53 d, $^2J_{HH}$ 13.8
H_A	4.85 d, $^2J_{HH}$ 15.6	5.25 dd, $^2J_{HH}$ 15.2, $^2J_{PH}$ 2.0
H_E	5.22 d, $^2J_{HH}$ 13.9	4.93 d, $^2J_{HH}$ 13.8
H_D	5.62 d, $^2J_{HH}$ 13.7	5.79 d, $^2J_{HH}$ 14.0

the presence of two phosphorus atoms, stereogenic in the *anti* form of DCP.

In DMSO six ^{31}P NMR signals of different intensity were observed at −28.0, −27.8, −27.7, −26.8, −26.6 and –26.5 ppm, with similar values of $^1J_{PtP}$ (ca. 3400 Hz). This pattern is reproducible for different preparations and it did not change at a daily observation for 15 days. The six signals are probably due to combinations of the three rotameric forms of the ligand DCP.

Crystals of complex **2** suitable for X-ray crystal structure determination were obtained from acetone and ether, (Fig. 6 and Tables 4 and 5).

The asymmetric unit is formed by a Pt complex and a co-crystallized water molecule. The complex presents a slightly distorted square-planar geometry, with the metal center bound through the phosphorous atom to two DCP (both in *anti* conformation) and two chlorine atoms in *cis* position; the distortion from the ideal geometry is mainly due to the steric encumbrance of the organic ligands. The Pt atom is located 0.016 Å above the least-squares plane formed by Cl1, Cl2, P1, P2 atoms. As for Pt−P and Pt−Cl distances, they are in good agreement with the mean values of 2.25(4) and 2.36(4) Å calculated for analogous complexes (1959 hits in the Cambridge Structural Database (CSD). Due to the lack of good hydrogen bonding donors, the crystal packing of the structure is characterized by the presence of a number of weak C−H…O interactions, listed in Table 5. The only exception is the Cl7…Cl9 interaction with an inter-halogen distance that is less than the sum of the van der Waals radii (Table 5). For this type of interactions there are two preferred geometries, according to the values assumed by θ_1 (R1−X…X) and θ_2 (X…X−R2) angles the first occurs when $\theta_1 = \theta_2$, while the second occurs when $\theta_1 \approx 180^\circ$ and $\theta_2 \approx 90^\circ$ [35]. In the present case the second arrangement has been found, the C16−Cl7…Cl9 and Cl7…Cl9−C18 angles measuring 172° and 100°, respectively. The co-crystallized water molecule is loosely bound, not being involved in any hydrogen bonding interaction.

In order to obtain the mixed phosphine complex *cis*-[$PtCl_2$(DCP)(PTA)] (**1**), bearing two dichloroacetic groups, we exploited the reaction of complex *cis*-[$PtCl_2(PTA)_2$] with one equivalents of DCP, a stronger nucleophile, in CH_3CN. The ^{31}P NMR of **1** in acetone showed two broad signals at −28.0 ppm ($^1J_{PtP}$ ca. 3393 Hz) and –53.4 ppm ($^1J_{PtP}$ 3118 Hz) corresponding to coordinated DCP and coordinated PTA respectively.

The cationic complex **3**, containing three DCP ligands (corresponding to a total of six dichloroacetyl residues), was obtained by adding solid K_2PtCl_4 to a solution containing three eq. of DCP in CH_3CN, or alternatively by adding one eq. of DCP to complex **2**.

The identity of complex **3** was confirmed by ESI-MS giving a single peak corresponding to M^+ at 1332 *m/z*. The ^{31}P NMR in DMSO showed a very broad signal centered at −27.6 ppm with $^1J_{PtP}$ = ca. 3362 Hz.

Complex **4**, containing two DCP ligands and two dichloroacetate ions as anionic ligands, carrying a total of six dichloroacetyl groups,

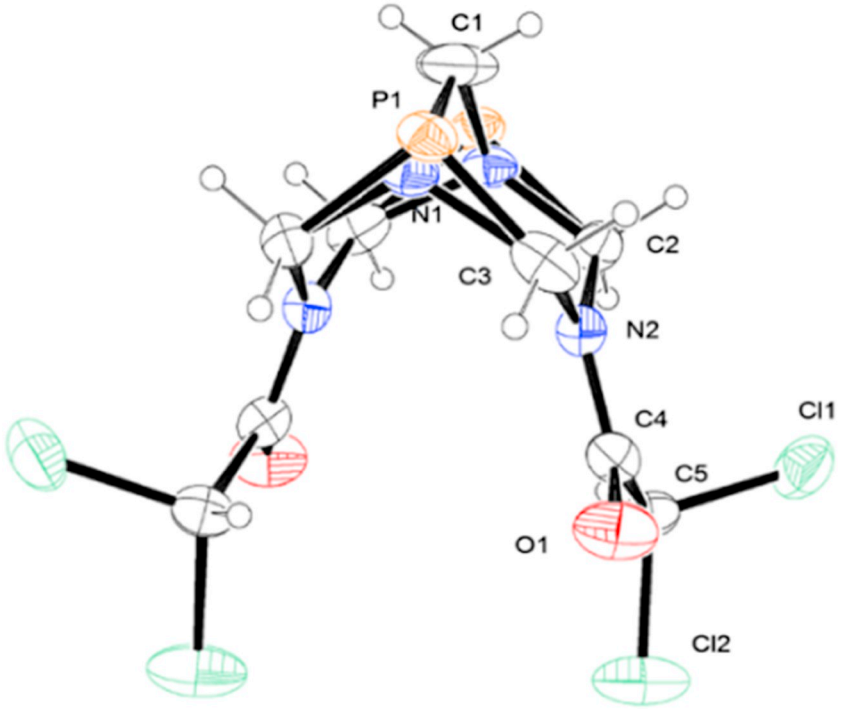

Fig. 4. ORTEP-III view and atom numbering scheme for DCP [34].
Thermal ellipsoids are drawn at the 40% probability level.

Table 2
Selected bond distances and angles (Å,°) for DCP.

Bond distances	(Å)	Bond angles	(°)
C4−O1	1.225(4)	N2−C4−C5	117.5(3)
C5−Cl2	1.751(4)	C4−C5−Cl1	109.3(3)
C5−Cl1	1.781(4)	N2−C4−O1	123.4(3)
C1−P1	1.652(4)	C4−C5−Cl2	110.7(2)
C1−N1	1.633(9)	C5−C4−O1	119.0(3)
		Cl1−C5−Cl2	109.8(2)

Table 3
Structural parameters of hydrogen bonds (Å,°) for DCP.

D−H…A	D−H	D…A	H…A	D−H…A
C2−H…O1^{i}	1.00(4)	3.398(5)	2.50(4)	149(3)
C5−H…O1^{i}	0.87(5)	3.128(5)	2.27(5)	173(4)
C3−H…O1^{ii}	0.90(4)	3.431(5)	2.58(4)	157(4)

Equivalent positions: (i) x,1-y, z + 1/2; (ii) 1-x,1-y,1-z.

was prepared in two steps from $[PtCO_3(DMSO)_2]$ (Scheme 2). The ^{31}P NMR of the carboxylate complex **4** showed two broad signals in DMSO (−36.1, $^{1}J_{PtP}$ = 3501 Hz and − 37.7, $^{1}J_{PtP}$ = 3467 Hz), and a single signal in acetone (−36.6 $^{1}J_{PtP}$ = 3577 Hz).

2.2.2. Coordination of DCP to Pd(II)

Although the use of Pd complexes in medicinal chemistry was largely less explored than Pt, some Pd complexes have revealed a promising cytotoxic action on several tumor cell lines [36]. For example, Pd(II) complexes containing PTA were reported, with IC50 values comparable to that of cisplatin on tumor cells A2780 (cisplatin-sensitive ovarian carcinoma), showing at the same time high cytotoxicity on the A2780*cis* line (cisplatin-resistant) [37–38].

The Pd complex *cis*-$[PdCl_2(DCP)_2]$ (**5**), (Fig. 7), analogue of the above described Pt complex **2**, was easily prepared in 88% yield by treating $PdCl_2$ with 2 eq. of DCP in CH_2Cl_2. The *cis* geometry is confirmed by the IR spectrum which showed the diagnostic pair of Pd−Cl stretching at 366 e 356 cm^{-1}. In ESI-MS a peak was observed at 935, corresponding to M + Na^+.

The cationic Pd complex **6**, (Fig. 7), was obtained from $PdCl_2$, treated in CH_2Cl_2 with 3 eq. of DCP. Although the ^{31}P and ^{1}H NMR are not very informative due to a diffuse signals broadening, the identity of **6** was unequivocally confirmed by ESI-MS where a single peak was observed, corresponding to M^+ at 1242 *m/z*.

2.2.3. Synthesis of [$RuCl_2(\eta^6$p-cymene)(DCP)] (7), a Ru(II) complex

Another metal ion belonging to Pt group metals, Ru^{2+} has been studied for its peculiar properties in the anticancer action: it was reported that Ru(II) complexes with PTA, named "RAPTA" series, are provided of anti-metastatic activity [39–40]. Ru complexes of alkylPTA [41–43] and Ru(II) DAPTA complexes [44], provided of anti-proliferative activity, were also described.

We prepared [$RuCl_2(\eta^6$p-cymene)(DCP)], complex **7**, (Fig. 8), by treating the known chloro-bridged dimeric complex [$Ru_2Cl_4(\eta^6$p-cymene)$_2$] with two equivalents of DCP in CH_3CN.

Alternatively complex **7** can be obtained also by acylation of Ru-coordinated PTA in [$RuCl_2(\eta^6$p-cymene)(PTA)], although with a low yield (30%). The ^{31}P NMR of complex **7** in DMSO showed three signals of the three rotamers at −13.0 ppm −7.8, −7.1 in about 1:9:3 ratio, the same found also in ^{1}H NMR, which displayed for the $CHCl_2$ group two close signals at 7.09 and 7.10 ppm due to the *anti*, major rotamer, a signal at 7.29 (*syn*), and finally another singlet at 7.42 ppm (*syn*). In acetone, where **7** is scarcely soluble, a single signal was observed in ^{31}P NMR at −8.1 ppm and in ^{1}H NMR only two signals belonging to the inequivalent $CHCl_2$ of the *anti* form were found at 6.82 and 6.90 ppm.

2.2.4. Synthesis of [$Re(CO)_3$(o-phen)DCP]NO_3 (8), a Re(I) complex

In a recent paper, a series of cationic complexes of Re(I) [Re$(CO)_3$(*o*-phen)$(PR_3)]^+$ (*o*-phen = 1,10-phenanthroline; PR_3 = PTA, THMP, DAPTA) have been considered for photoactivated anticancer activity in vitro [45]. The best performance was observed with [Re$(CO)_3$(*o*-phen)(DAPTA)]$^+$. We prepared the DCP analogue (**8**), (Fig. 9).

The precursor [$Re(CO)_3$(*o*-phen)Cl], prepared as described [46], was dissolved in CH_3CN and converted in the solvento-complex [Re$(CO)_3$(*o*-phen)$(CH_3CN)]NO_3$ by adding $AgNO_3$. DCP was then added for replacing the Re coordinated CH_3CN. The final yellow solution contained complex **8**, [$Re(CO)_3$(*o*-phen)(DCP)]NO_3, which was recovered in high yield by precipitation with ether.

The ESI-MS of complex **8** showed the M^+ peak at 816 *m/z*. The NMR characterization confirmed the complex identity.

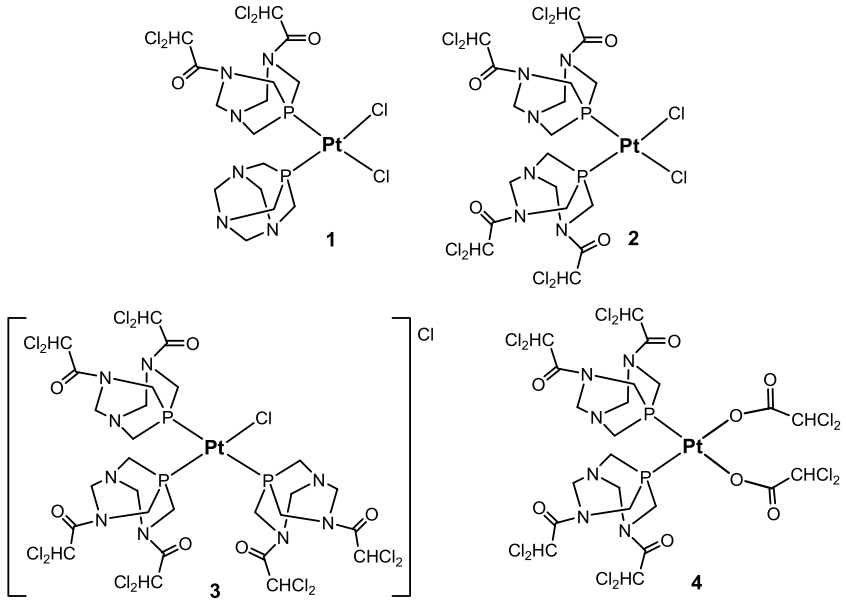

Fig. 5. Platinum complexes of DCP: *cis*-$[PtCl_2(DCP)(PTA)]$ (**1**), *cis*-$[PtCl_2(DCP)_2]$ (**2**), *cis*-$[PtCl(DCP)_3]Cl$ (**3**) and *cis*-$[Pt(DCA)_2(DCP)_2]$ (**4**).

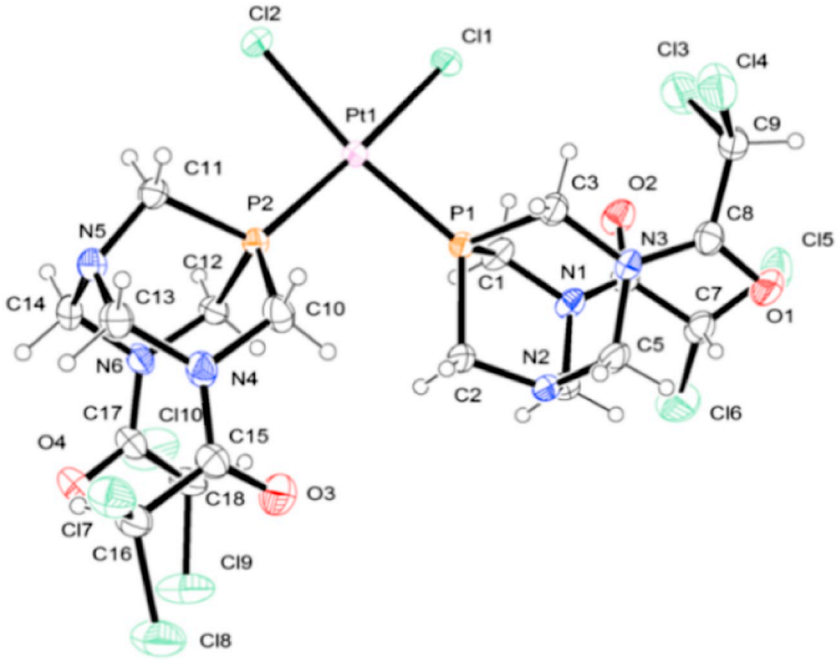

Fig. 6. ORTEP-III view and atom numbering scheme for complex **2** [34]. Thermal ellipsoids are drawn at the 40% probability level. The co-crystallized water molecule is not shown for clarity.

Table 4
Selected bond distances and angles (Å,°) for complex **2**.

Bond distances	(Å)	Bond angles	(°)
Pt1−P1	2.231(1)	P1−Pt1−P2	98.36(5)
Pt1−P2	2.236(2)	P1−Pt1−Cl1	85.20(5)
Pt1−Cl1	2.357(2)	P2−Pt1−Cl2	89.55(5)
Pt1−Cl2	2.348(1)	P2−Pt1−Cl1	174.58(5)
		P1−Pt1−Cl2	171.75(5)
		Cl1−Pt1−Cl2	87.08(5)

Table 5
Structural parameters of hydrogen bonds (Å, °) for **2**.

D−H…A	D−H	D…A	H…A	D−H…A
C3−H…Cl3	0.97	3.325(7)	2.57	134
C2−H…O1W^{i}	0.97	3.524(9)	2.61	156
C18−H…O1W^{i}	0.98	3.238(9)	2.41	142
C5−H…O1^{ii}	0.97	3.494(6)	2.59	155
C4−H…O1^{ii}	0.97	3.482(6)	2.58	154
C7−H…O1^{ii}	0.98	3.263(7)	2.38	148
C9−H…O4^{iii}	0.98	3.053(8)	2.21	143
C12−H…O2^{iv}	0.97	3.134(6)	2.31	141
Short Cl…Cl contact:				
Cl7…Cl9^{v}		3.340(2)		

Equivalent positions: (i) -x, -y-1, -z; (ii) -x, -y-1, -z-1; (iii) x, y, z-1; (iv) -x, -y, -z; (v) x + 1, y, z.

2.2.5. Synthesis of [AuCl(DCP)] (9), a Au(I) complex

Several gold species provided with antiproliferative activity were reported, including phosphine complexes. Their mechanism of action, different from that of the platinum-based drugs, seems to be due to alterations of mitochondrial functions triggered by TxR (thioredoxin reductase) inhibition [47–50].

The complexes [AuCl(PTA)] [51] and [AuCl(DAPTA)] [31] were prepared by replacement of tetrahydrothiophene (tht) from [AuCl(tht)] with the appropriate phosphine. Analogously, the reaction of [AuCl (tht)] with DCP in CH_2Cl_2 gave complex [AuCl(DCP)], (**9**), in high yield, (Fig. 10). In DMSO the presence of the expected three rotamers was found, whose signals are well distinct in ^{31}P NMR at −24.8, −19.3 and –18.4 ppm, in a 1:12.5:1 ratio, and partially overlapped in ^{1}H and ^{13}C NMR. In acetone a single form was detected (^{31}P NMR −19.2 ppm).

2.3. Anti-proliferative activity

The anti-proliferative activity of the new ligand DCP and of the complexes **1–9** was assayed on the A2780 (sensitive to cisplatin) and A2780*cis* (cisplatin resistant) ovarian cancer cell lines (both growing attached on the tissue culture flask and representative of solid tumors), and on the erythroleukemia K562 cell line (growing in suspension and representative of liquid tumors). The antineoplastic agent cisplatin was used as positive control in parallel cell cultures for each experiment. The obtained results are reported in Table 6.

Concerning the human ovarian cancer cell lines A2780 and A2780*cis*, while the known marked anti-proliferative activity of cisplatin (IC_{50} = 0.4 ± 0.1 μM) on A2780 and the cisplatin-resistance of the A2780*cis* (IC_{50} = 4.51 ± 0.7 μM) were both confirmed [52–54], all the here described new complexes demonstrated anti-proliferative activity on both cell lines, at different levels. When the results obtained using the A2780 cell line were comparatively analyzed, only complex **3** showed a relevant activity (IC_{50} = 0.78 ± 0.1 μM), comparable with cisplatin and stronger than the uncoordinated ligand DCP. On the cisplatin-resistant A2780*cis* cells, the noteworthy activity of the ligand DCP (IC_{50} = 0.94 ± 0.1 μM) was improved by Pt coordination in complexes **2**, **3** and **4** (IC_{50} = 0.09 ± 0.01, 0.32 ± 0.04, 0.62 ± 0.06 μM, respectively).

On the K562 cells the anti-proliferative effects of the complexes, compared with cisplatin (IC_{50} = 0.52 ± 0.1 M), were significantly different: **1**, **5**, **6**, **7** exhibited low activity (IC_{50} = 15–20 μM); **2**, **3**, **8** and **9** revealed intermediate activity (IC_{50} = 2–8 μM), whereas the complex **4** (IC_{50} = 0.58 ± 0.1 μM) showed an efficacy very similar to the positive control cisplatin and better than the free ligand DCP (3.98 ± 0.7 μM). These results seem to indicate that the association of DCP with Pt(II) produces the best performances. The activity of Pt complexes **1**, **2** and **3** on cisplatin-resistant cells seems to indicate that they act through a different mechanism from that of classical Pt anticancer drugs.

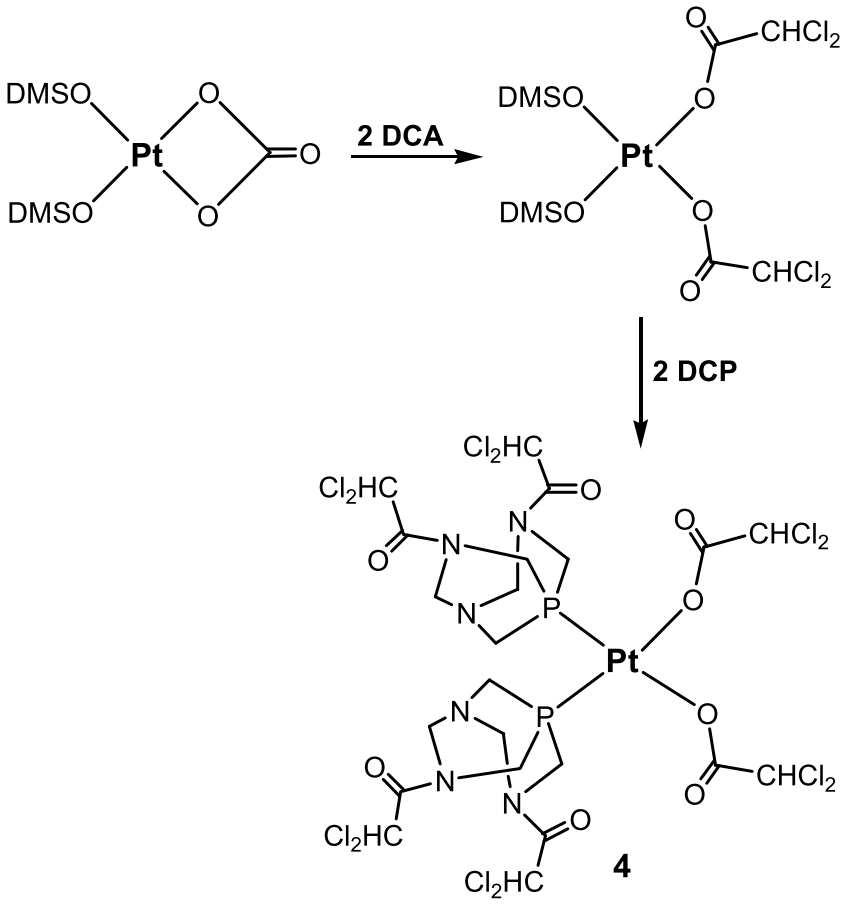

Scheme 2. Synthesis of *cis*-[Pt(DCA)$_2$(DCP)$_2$] (**4**).

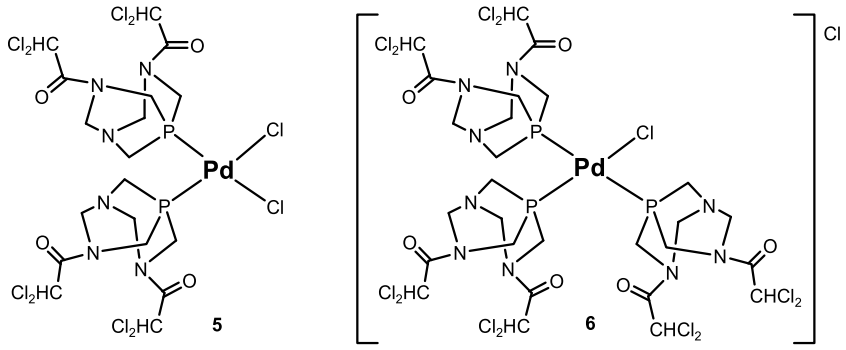

Fig. 7. Pd complexes of DCP: *cis*-[PdCl$_2$(DCP)$_2$] (**5**) and *cis*-[PdCl(DCP)$_3$]Cl (**6**).

The complexes containing DCP and non-platinum metal ions (**5**–**9**) were found not very active.

2.4. Pro-apoptotic effects

To attest whether the anti-proliferative activity of the complexes is associated to the activation of the apoptotic pathway, all the complexes were comparatively assayed, using the Annexin V test and a Muse™ Cell Analyzer [55–56]. All the MUSE-plots are reported in the Supplementary material, and the summary of the data obtained is shown in Table 7. Each derivative, with the exception of the compound **7** on A2780 cells and **8** on K562 cells, induced clearly appreciable pro-apoptotic effects on the employed cell lines. We have performed the assays using concentrations able to induce anti-proliferative effects, previously determined.

On the A2780 cell line at 5 μM, the Pt complexes **2**, **3** and **4** were identified as the best inducers of apoptosis (ca 50%), although less efficient than cisplatin, when used at the same concentration (77%). On the A2780*cis* cell line, cisplatin is not very active (as expected), while the Pt complexes **2**, **3** and **4** were found very active (51.60, 68.75 and 45.50 respectively) at the same dose (1 μM).

On K562 cells, the cisplatin proapoptotic activity is not very marked. Considering the values at 5 μM, all the Pt complexes (except **4**, that was among the most active when antiproliferative activity was considered, see Table 6) are more active than cisplatin. Surprisingly, the complexes containing Pd (**5** and **6**), Ru (**7**) and Au (**9**) showed a remarkable activity, while the Re complex (**8**) is nearly inactive. The free ligand DCP is less proapoptotic than its metal complexes on the three lines.

There is a good agreement between the antiproliferative activity

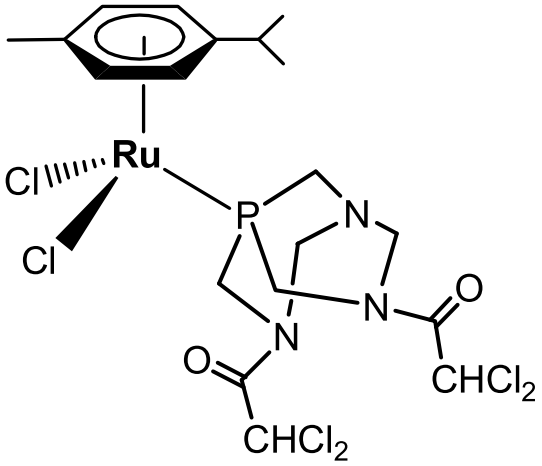

Fig. 8. Ruthenium complex of DCP, [$RuCl_2(\eta^6$*p*-cymene)(DCP)] (**7**).

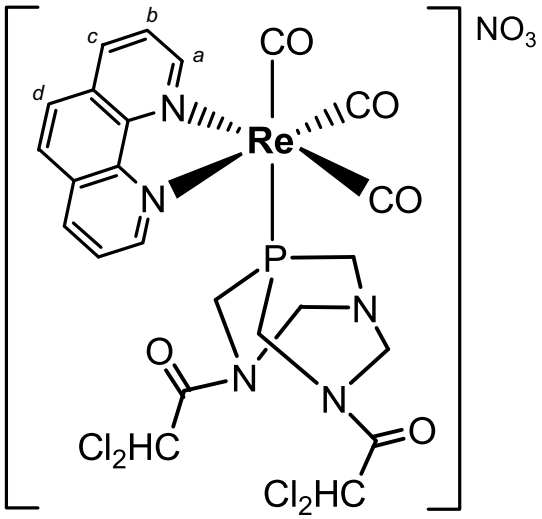

Fig. 9. Rhenium complex of DCP, [Re(*o*-phen)$(CO)_3$(DCP)]NO_3 (**8**).

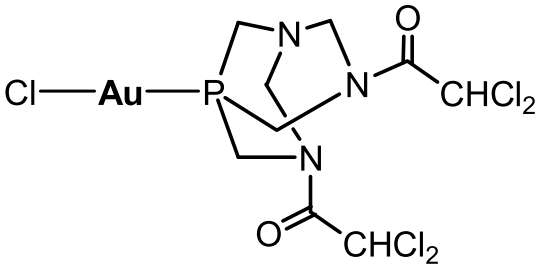

Fig. 10. Gold complex of DCP [AuCl(DCP)] (**9**).

(Table 6) and the proapoptotic effects (Table 7) on the ovarian cancer cell lines and Pt complexes **2**, **3** and **4** show the best activity when both tests are considered. Remarkably, the complex **4** (very active on inhibition of cell growth and induction of apoptosis when A2780 and A2780*cis* are employed) displayed, on K562 cells, a very high antiproliferative activity (0.58 ± 0.1 μM), associated with very poor proapoptotic effects.

The mixed PTA/DCP complex **1** shows negligible activity in both tests. Comparing the activity e.g. on A2780 of *cis*-[$PtCl_2(PTA)_2$] (IC_{50} > 50 μM [57]) *cis*-[$PtCl_2$(PTA)(DCP)] (**1**, IC_{50} = 7.99 ± 0.1 μM) and *cis*-[$PtCl_2(DCP)_2$] (**2**, IC_{50} = 4.22 ± 0.3 μM), a positive trend is appreciable with the increasing of DCP.

The ability of inducing differentiation on the K562 cells was also tested, in comparison with cisplatin, whose activity was reported [58], but all the new species were found inactive (data not shown).

Table 6
Effects of the complexes on the proliferation of A2780, A2780*cis* and K562 cells. The inhibition of cell growth is represented as IC_{50}.

Complex	IC_{50}(μM)A2780	IC_{50}(μM)A2780*cis*	IC_{50}(μM)K562
Cisplatin	0.40 ± 0.1	4.51 ± 0.7	0.52 ± 0.1
DCP	4.74 ± 0.6	0.94 ± 0.1	3.98 ± 0.7
1	7.99 ± 0.1	6.39 ± 0.4	23.04 ± 0.9
2	4.22 ± 0.3	0.09 ± 0.01	1.88 ± 0.2
3	0.78 ± 0.1	0.32 ± 0.04	1.96 ± 0.4
4	3.26 ± 0.3	0.62 ± 0.06	0.58 ± 0.1
5	5.27 ± 0.9	4.83 ± 0.8	14.84 ± 0.7
6	4.49 ± 0.8	3.60 ± 0.2	15.33 ± 1.3
7	9.95 ± 0.9	6.82 ± 0.03	15.12 ± 1.4
8	2.42 ± 0.2	6.65 ± 0.5	8.45 ± 0.3
9	4.17 ± 0.2	6.78 ± 0.2	4.01 ± 0.2

Table 7
Pro-apoptotic effects of DCP and complexes **1–9** on human A2780, A2780*cis* and K562 cells.

Sample	A2780		A2780*cis*		K562	
	Live cells (%)	Apoptotic cells (%)	Live cells (%)	Apoptotic cells (%)	Live cells (%)	Apoptotic cells (%)
C-	91.90	7.85	89.50	8.80	96.30	3.70
CisPt 0.5 μM	81.30	18.10	89.75	9.60	95.05	4.15
CisPt 1.0 μM	59.30	40.20	85.55	11.80	79.45	19.90
CisPt 5.0 μM	22.00	77.25	72.40	28.20	66.37	32.13
DCP 0.1 μM			68.90	29.00		
DCP 0.5 μM			83.75	15.15		
DCP 1.0 μM	91.50	8.00	72.80	26.70	91.20	8.55
DCP 5.0 μM	59.60	39.55			56.72	35.40
DCP 10 μM	46.70	50.05			64.50	43.00
1 1.0 μM	91.85	7.50	82.87	13.29	79.15	20.65
1 5.0 μM	69.30	26.55	66.71	30.17	49.90	49.20
1 10 μM	76.65	21.20	60.63	36.31	16.30	83.70
2 0.1 μM			80.25	18.80		
2 0.5 μM			58.25	41.15		
2 1.0 μM	79.85	20.00	47.20	51.60	95.70	4.05
2 5.0 μM	43.80	52.90			57.40	41.75
2 10 μM	38.70	58.60			15.34	84.59
3 0.05 μM			88.05	11.05		
3 0.1 μM			81.65	17.90		
3 0.5 μM					74.71	24.89
3 1.0 μM	67.60	29.70	26.05	68.75	60.30	39.65
3 5.0 μM	29.55	66.20			40.45	59.40
3 10 μM	47.20	49.95				
4 0.1 μM			69.85	28.25		
4 0.5 μM			51.10	44.40		
4 1.0 μM	88.15	11.35	53.55	45.50	95.20	4.45
4 5.0 μM	44.40	50.35			95.30	4.70
4 10 μM	39.95	49.95			81.75	18.25
5 1.0 μM	91.95	7.50	84.17	14.45	73.13	26.70
5 5.0 μM	69.50	28.05	57.79	40.58	25.70	74.30
5 10 μM	58.95	37.05	19.38	79.80	20.93	79.01
6 1.0 μM	91.85	7.05	82.05	16.50	65.89	33.54
6 5.0 μM	71.10	25.25	64.23	34.31	37.45	62.30
6 10 μM	66.99	31.50	37.68	60.67	31.45	68.15
7 1.0 μM	90.25	8.95	84.15	14.94	82.80	16.91
7 5.0 μM	82.90	16.20	60.49	34.53	52.70	45.85
7 10 μM	87.40	11.60	47.47	47.63	44.65	54.95
8 1.0 μM	87.55	10.85	81.45	17.31	89.93	8.97
8 5.0 μM	71.65	27.40	66.85	32.39	93.77	6.08
8 10 μM	37.40	61.45	52.54	47.10	89.43	10.09
9 1.0 μM	92.05	6.90	82.08	17.21	86.34	12.90
9 5.0 μM	63.05	33.15	48.72	43.44	44.14	54.92
9 10 μM	76.35	21.30	38.22	60.41	15.50	84.40

3. Experimental section

3.1. General procedures

All the manipulations were carried out in air unless otherwise noted. Commercial starting materials K_2PtCl_4, $PdCl_2$, $[Ru_2Cl_4(\eta^6p\text{-cymene})_2]$, $HAuCl_4$ and all the solvents and reagents were purchased and used without further purification. PTA [59], *cis*-$[PtCl_2(PTA)_2]$ [60], *cis*-$[Pt(DCA)_2(DMSO)_2]$ [57], $[RuCl_2(\eta^6p\text{-cymene})PTA]$ [41–43] $[Re(CO)_3(o\text{-phen})Cl]$ [46], [AuCl(tht)] [61] were prepared as described in the literature.

Elemental analyses were determined using a Carlo Erba instrument model EA1110. Mass spectra were recorded by an ESI single quadrupole mass spectrometer Waters ZQ 2000 (Waters instruments UK) and in each case the isotope pattern fitted the calculated (see Supplementary material). NMR spectra were recorded on a Varian Gemini 300 MHz spectrometer (^{1}H at 300 MHz, ^{13}C at 75.43 MHz, ^{31}P at 121.50 MHz) or a Varian Mercury Plus (^{1}H at 400 MHz, ^{13}C at 100.58 MHz, ^{31}P at 161.92 MHz). The ^{13}C and ^{31}P spectra were run with proton decoupling, ^{13}C signals are reported in ppm relative to external tetramethylsilane (TMS), ^{31}P signals are reported in ppm relative to an external 85% H_3PO_4 standard. The NMR spectra were recorded on fresh solutions (10–60 min) and the stability of the complexes in DMSO was routinely checked by the re-observation of ^{31}P NMR spectra after 24 h.

3.2. Synthesis and characterization of DCP

PTA (500 mg, $3.18\cdot10^{-3}$ mol, MW 157.15 g/mol) was dissolved in a Na_2CO_3 solution (0.12 M, pH 11.7, 8 mL) and 10 mL of CH_2Cl_2 were added. The emulsion was then put under inert atmosphere and dichloroacetic anhydride (2.3 mL, $1.4\cdot10^{-2}$ mol, MW 239.9 g/mol, 4.4 eq.) was added dropwise under vigorous stirring, triggering the formation of a white precipitate at the interphase. The reaction mixture was kept under stirring at room temperature for an hour and then was filtered to recover the solid product which was carefully washed with water and ethanol to remove traces of sodium dichloroacetate, then dried under the vacuum on P_2O_5.

DCP was obtained as a white powder (872 mg, $2.38\,10^{-3}$ mol, MW 367.00 g/mol, yield 74.5%).

^{1}H NMR (DMSO-d_6)/COSY: δ = 3.53 ppm (dd, $^2J_{HH} = {}^2J_{PH}$ = 15.6 Hz, 1H, A), 3.59 ppm (d, $^2J_{PH}$ = 10.8 Hz, 2H, C), 3.93 ppm (dd, $^2J_{HH} = {}^2J_{PH}$ = 13.2 Hz, 1H, B), 4.18 ppm (d, ^2J = 13.4 Hz, 1H, D), 4.52 ppm (m, 2H, E, B′), 4.76 ppm (d, ^2J = 15.6 Hz, 1H, A′), 5.09 ppm (d, ^2J = 14.0 Hz, 1H, E′), 5.27 ppm (d, ^2J = 13.2 Hz, 1H, minor), 5.48 ppm (d, ^2J = 13.4 Hz, 1H, D′), 7.04 ppm (s, $CHCl_2$, 1H, major) and 7.15 ppm (s, $CHCl_2$, 1H, major), 7.18 ppm (s, $CHCl_2$ minor), 7.28 ppm (s, $CHCl_2$ minor). ^{1}H NMR (DMSO-d_6): at 80 °C single broad peak for $CHCl_2$ at 7.12 ppm. General broadening of the other signals. ^{31}P NMR (DMSO-d_6): δ = −78.5 ppm (s), −68.8 ppm (s), −68.4 ppm (s), estimated intensity ratio 1:7:1. At 120 °C ca −70 ppm (broad signal). ^{13}C NMR/DEPT-HETCOR (DMSO-d_6) δ = 38.0 ppm (d, CH_2P, $^1J_{PC}$ = 28.4 Hz, major), 40.8 ppm (d, CH_2P, $^1J_{PC}$ = 29.2 Hz, minor), 41.6 ppm (d, CH_2P, $^1J_{PC}$ = 27.5 Hz, major), 44.7 ppm (d, CH_2P, $^1J_{PC}$ = 15.3 Hz, major), 62.8 ppm (s, NCH_2N, major), 63.6 ppm (s, NCH_2N, minor), 65.2 ppm e 65.4 ppm (s, $CHCl_2$, minor), 65.6 ppm (s, $CHCl_2$, major), 65.8 ppm (s, NCH_2N, major), 66.1 ppm (s, $CHCl_2$, major), 161.4 ppm (s, CO minor), 161.7 ppm (s, CO minor) 161.6 ppm and 162.0 (s, CO, major). ^{1}H NMR (acetone-d_6)/COSY: δ = 3.60 ppm (dt, $^2J_{HH} = {}^2J_{PH}$ = 15.1 Hz, $^4J_{HH}$ = 2.3 Hz, 1H, A), 3.78 ppm (d, $^2J_{PH}$ = 11.3 Hz, 2H, C), 4.15 ppm (dt, $^2J_{HH} = {}^2J_{PH}$ = 14.7 Hz, $^4J_{HH}$ = 2.3 Hz, 1H, B), 4.32 ppm (d, $^2J_{HH}$ = 13.7 Hz, 1H, D), 4.63 ppm (d, $^2J_{HH}$ = 15.0 Hz, 1H, B′), 4.78 ppm (d, J_{HH} = 13.9 Hz, 1H, E), 4.85 ppm (d, J_{HH} = 15.6 Hz, 1H, A′), 5.22 ppm (d, $^2J_{HH}$ = 13.9 Hz, 1H, E′), 5.62 ppm (d, $^2J_{HH}$ = 13.7 Hz, 1H, D′), 6.85 ppm (s, $CHCl_2$, 1H), 6.88 ppm (s, $CHCl_2$, 1H). ^{31}P NMR (acetone): −69.23 ppm. ^{31}P NMR (acetonitrile): −68.6 ppm. ^{31}P NMR (DMF): −77.4 ppm (s), −67.5 ppm (s), −67.1 ppm (s) estimated intensity ratio ca 1:7:1. ESI-MS: m/z = 368 ($MH^+ = C_9H_{13}Cl_4N_3O_2P$). Anal. Calcd. for $C_9H_{12}Cl_4N_3O_2P$: C 29.45, H 3.30, N 11.45; found C 29.38, H 3.45, N 11.42. The crystallographic structure of **1** was determined on crystals grown in acetone (see Tables 2 and 3, Fig. 4).

3.3. Coordination of DCP to metal ions

3.3.1. Synthesis of cis-$[PtCl_2(DCP)_2]$ (2)

Solid K_2PtCl_4 (100 mg, $2.41\cdot10^{-4}$ mol, MW 415.0 g/mol) was added to a solution of DCP (177 mg, $4.82\cdot10^{-4}$ mol, MW 367.0 g/mol, 2 eq.) in 60 mL of CH_3CN. The suspension was left under stirring for 18 h. The obtained colorless solution, taken to dryness by rotary evaporator left a white solid residue which was washed with water (to remove the side product KCl), filtered and dried under vacuum over P_2O_5 (190 mg, $1.9\cdot10^{-4}$ mol, MW 1000.0 g/mol, yield 79%).^{1}H NMR (DMSO-d_6): δ = 3.85–5.45 ppm (10H of DCP), 6.83 ppm and 6.97 ppm and 7.18 ppm (3 s, 2H, $CHCl_2$). ^{31}P NMR (DMSO-d_6): −28.0 ppm ($^1J_{PtP}$ = ca 3400 Hz), −27.8 ppm ($^1J_{PtP}$ = ca 3400 Hz), −27.7 ppm ($^1J_{PtP}$ = ca 3400 Hz), −26.8 ppm ($^1J_{PtP}$ = ca 3454 Hz), −26.6 ppm ($^1J_{PtP}$ = ca 3454 Hz) and –26.5 ppm ($^1J_{PtP}$ = ca 3454 Hz). ^{31}P NMR (acetone): δ = −27.3 ppm (s, $^1J_{PtP}$ = 3389 Hz) and –27.2 ppm (s, $^1J_{PtP}$ = 3341 Hz). ^{31}P NMR (acetonitrile): δ = −28.1 (s, $^1J_{PtP}$ = 3395 Hz). Anal. Calcd. for $C_{18}H_{24}Cl_{10}N_6O_4P_2Pt$: C 21.61, H 2.42, N 8.40; found C 21.63, H 2.40, N 8.47. The crystallographic structure of **2** was determined on crystals grown in acetone and ether (see Tables 4 and 5, Fig. 6).

3.3.2. Synthesis of cis-$[PtCl_2(PTA)(DCP)]$ (1)

DCP (127 mg, $3.45\cdot10^{-4}$ mol, MW 367.0 g/mol) was dissolved in 57 mL of CH_3CN and added to a suspension of *cis*-$[PtCl_2(PTA)_2]$ (200 mg, $3.45\cdot10^{-4}$ mol, MW 579.9 g/mol) in 33 mL of CH_3CN + 13 mL of CH_3OH. During 48 h stirring, the suspension turned to a clear colorless solution which was taken to dryness by rotary evaporator. The white solid residue was suspended in water, left under stirring for 18 h and finally filtered. It was then dried under vacuum over P_2O_5 (117 mg, $1.48\cdot10^{-4}$ mol, MW 790.1 g/mol, yield 43%).

^{1}H NMR (300 MHz, acetone-d_6): δ = 4.17 ppm (d, 2H, $^2J_{HH}$ = 18 Hz), 4.4–4.7 ppm (m, 11 H, DCP + PTA), 4.85 ppm (d, 2H, $^2J_{HH}$ = 18 Hz), 5.2–5.7 ppm (m, 7H, DCP), 6.78 and 6.83 (2s, 2H, $CHCl_2$). ^{31}P NMR (acetone): δ = −53.4 ppm (bs, $^1J_{PtP}$ = 3118 Hz), −28.0 ppm (bs, $^1J_{PtP}$ = 3393 Hz). ^{31}P NMR (DMSO): δ = −51.1 ppm (bs, $^1J_{PtP}$ = 3131 Hz), −27.4 ppm (bs, $^1J_{PtP}$ = 3400 Hz, major), −26.2 ppm (bs, $^1J_{PtP}$ = 3400 Hz, minor). IR nujol: 398 and 374 cm^{-1} ν Pt-Cl *cis*, 446 and 435 cm^{-1} ν Pt-P. Anal. Calcd. for $C_{15}H_{24}Cl_6N_6O_2P_2Pt$: C 22.79, H 3.06, N 10.64; found C 22.66, H 2.98, N 10.62.

3.3.3. Synthesis of $[PtCl(DCP)_3]Cl$ (3)

DCP (100 mg, $2.72\cdot10^{-4}$ mol, MW 367.00 g/mol, 3 eq.) was dissolved in 30 mL of CH_3CN. Solid K_2PtCl_4 (38 mg, $9.15\cdot10^{-5}$ mol, MW 415.1 g/mol) was added to the solution and left under stirring at room temperature for 18 h. The suspension was taken to dryness by rotary evaporator. The white solid residue was washed with water, filtered and dried under vacuum over P_2O_5 (79 mg, $5.78\cdot10^{-5}$ mol, MW 1367.0 g/mol, yield 63%).

^{1}H NMR (DMSO-d_6): δ = 3.8–5.5 ppm (10H of DCP), 7.0 ppm and 7.15 ppm and 7.3 ppm (3s, 2H, $CHCl_2$). ^{31}P NMR (DMSO-d_6): δ = −27.6 ppm (br) with $^1J_{PtP}$ = ca. 3362 Hz. ESI-MS: m/z = 1332 ($M^+ = C_{27}H_{36}Cl_{13}N_9O_6P_3Pt$). Anal. Calcd. for $C_{27}H_{36}Cl_{14}N_9O_6P_3Pt$: C 23.71, H 2.65, N 9.22; found C 23.81, H 2.70, N 9.29.

3.3.4. Synthesis and characterization of cis-$[Pt(DCA)_2(DCP)_2]$ (4)

cis-$[Pt(DCA)_2(DMSO)_2]$ (94 mg, $1.55\cdot10^{-4}$ mol, MW 607.2 g/mol) was suspended in 5 mL of acetone and DCP (114 mg, $3.1\cdot10^{-4}$ mol, 367.00 g/mol, 2 eq.) dissolved in 15 mL of CH_3CN was added dropwise. After stirring for an hour and a half at room temperature, the volume of the solution was reduced, leaving a white precipitate which was

filtered, washed with small portions of ether and finally dried under vacuum over P_2O_5 (82 mg, $6.92 \cdot 10^{-5}$ mol, MW 1184.9 g/mol, yield 45%).

^{1}H NMR (300 MHz, DMSO-d_6): δ = 4.0–5.5 ppm (m, 20H), 5.9 and 6.15 ppm (bs, $CHCl_2$ of DCA, 2H), 6.92 ppm, 7.07 ppm and 7.3 ppm (3 s, 4H, $CHCl_2$). ^{31}P NMR (DMSO): δ = −37.7 ppm (s, $^1J_{PtP}$ = 3467 Hz), −36.1 ppm (s, $^1J_{PtP}$ = 3501 Hz). ^{1}H NMR (400 MHz, acetone-d_6): δ = 4.2–5.7 ppm (m, 20H), 6.18 ppm ($CHCl_2$ of DCA, 2H), 6.75 ppm and 6.90 ppm (2 s, 4H, $CHCl_2$). ^{31}P NMR (acetone): δ = −36.6 ppm (s, $^1J_{PPt}$ = 3577 Hz). Anal. Calcd. for $C_{22}H_{26}Cl_{12}N_6O_8P_2Pt$: C 22.29, H 2.21, N 7.09; found C 21.31, H 2.20, N 6.99.

3.3.5. Synthesis and characterization of cis-[$PdCl_2$(DCP)$_2$] (5)

A DCP suspension (415 mg, 1.1310^{-3} mol, MW 367.0 g/mol, 2 eq.) in 10 mL of CH_2Cl_2 was added under nitrogen to $PdCl_2$ (100 mg, $5.64 \cdot 10^{-4}$ mol, MW 177.3 g/mol) suspended in 20 mL of CH_2Cl_2. The resulting brown/red solution was kept under stirring overnight. The yellow precipitate was then filtered and dried under vacuum over P_2O_5 (452 mg, $4.96 \cdot 10^{-4}$ mol, MW 911.3 g/mol, yield 88%).

^{1}H NMR (DMSO-d_6, 300 MHz) 4–5.5 ppm (10H of DCP), 6.87 ppm and 7.09 ppm and 7.27 ppm (3 s, 2H, $CHCl_2$). ^{31}P NMR (DMSO): δ = −5.06, −5.29, −5.46, −5.93, −6.11, −6.34 ppm. ^{31}P NMR (acetone, 300 MHz): δ = −8.4 ppm (s).^{31}P NMR (CH_3CN): δ = −8.2 ppm (s). IR nujol: 366 and 356 cm^{-1} ν Pd-Cl *cis*, 442–426 cm^{-1} ν Pd-P. ESI-MS: *m/z* = 935 ($M + Na^+ = C_{18}H_{24}Cl_{10}NaN_6O_4P_2Pd$). Anal. Calcd. for $C_{18}H_{24}Cl_{10}N_6O_4P_2Pd$: C 23.71, H 2.65, N 9.22; found C 23.86, H 2.60, N 9.21.

3.3.6. Synthesis and characterization of [$PdCl$(DCP)$_3$]Cl (6)

Solid $PdCl_2$ (16 mg, $9.02 \cdot 10^{-5}$ mol, MW 177.3 g/mol) was added to a solution of DCP (100 mg, $2.71 \cdot 10^{-4}$ mol, MW 367.0 g/mol, 3 eq.) in 30 mL of CH_3CN. After 15 min $PdCl_2$ was completely dissolved. The pale yellow solution was left under stirring at room temperature for 18 h and then taken to dryness. The yellow solid residue of **6** was dried under vacuum over P_2O_5 (116 mg, $9.02 \cdot 10^{-5}$ mol, MW 1278.3 g/mol, yield 100%). ^{1}H NMR (DMSO-d_6, 400 MHz): δ = 3.83 ÷ 5.52 ppm (30H of DCP), 6.92 ppm (bs, 2H, $CHCl_2$), 7. 10 ppm (s, 2H, $CHCl_2$), 7.28 ppm (s, 2H, $CHCl_2$). ^{31}P NMR (DMSO): br s –5.0 ÷ −7.0 ppm. ESI-MS: *m/z* = 1242 ($M^+ = C_{27}H_{36}Cl_{13}N_9O_6P_3Pd$). Anal. Calcd. for $C_{27}H_{36}Cl_{14}N_9O_6P_3Pd$: C 25.35, H 2.84, N 9.86; found C 25.59, H 2.79, N 10.06.

3.3.7. Synthesis of [$RuCl_2$(η^6*p*-cymene)(DCP)] (7)

Complex **7** can be obtained in two ways: a) reaction of [Ru_2Cl_4(η^6*p*-cymene)$_2$] with DCP or b) acylation of [$RuCl_2$(η^6*p*-cymene)(PTA)] with dichloroacetic anhydride.

a) from [Ru_2Cl_4(η^6*p*-cymene)$_2$]: a DCP suspension (120 mg, $3.26 \cdot 10^{-4}$ mol, MW 367.0 g/mol, 2 eq.) in 20 mL of CH_3CN was added in small portions to a [Ru_2Cl_4(η^6*p*-cymene)$_2$] orange solution (100 mg, $1.63 \cdot 10^{-4}$ mol, MW 612.4 g/mol). After 18 h, an orange solid precipitated which was filtered, washed with CH_3CN and dried under vacuum over P_2O_5 (54 mg, $1.5 \cdot 10^{-4}$ mol, MW 673.2 g/mol, yield 46%).

b) from [$RuCl_2$(η^6*p*-cymene)(PTA)]: [$RuCl_2$(η^6*p*-cymene)(PTA)][20c] (140 mg, $3.02 \cdot 10^{-4}$ mol, MW 463.3 g/mol) was dissolved in a Na_2CO_3 solution (2 M, 2 mL) and 5 mL of CH_2Cl_2 were added. Under inert atmosphere, 162 µL of dichloroacetic anhydride ($9.06 \cdot 10^{-4}$ mol, MW 239.9 g/mol, 3 eq.) were added dropwise under vigorous stirring, and a precipitate immediately formed at the interphase. The reaction mixture was kept under stirring at room temperature for 4 h. The orange precipitate was then filtered, washed with water and ethanol and then dried under the vacuum on P_2O_5. [$RuCl_2$(η^6*p*-cymene)(DCP)] (**7**) was obtained as an orange powder (61 mg, $9.02 \cdot 10^{-5}$ mol, MW 673.2 g/mol, yield 30%). ^{1}H NMR/COSY (400 MHz, DMSO-d_6): δ = 1.11 and 1.12 ppm (2d, $^3J_{HH}$ = 6.83 Hz, 6H, isoprop), 1.93 ppm (s, 3H, p-CH_3), 2.59 ppm (ept, $^3J_{HH}$ = 6.83 Hz, 1H, isoprop), 3.9 ppm (m, 3H of NCH_2P groups), 4.28 ppm (m, 2H, NCH_2P and NCH_2N), 4.72 ppm (m, 2H, NCH_2P and NCH_2N), 5.14 ppm (m, 2H, NCH_2P and NCH_2N), 5.47 ppm (d, $^2J_{HH}$ = 13.5 Hz, 1H, NCH_2N), 5.87 ppm (m, 4H, aromatic), 7.09 ppm and 7.10 ppm (2 s, $CHCl_2$ of *anti* rotamer), 7.29 ppm and 7.42 ppm (2 s, $CHCl_2$ of *syn* rotamers *A* and *B*). ^{31}P NMR (121.44 MHz, DMSO): δ = −13.0 ppm (s), −7.8 ppm (s), −7.1 ppm (s), estimated ratio 1:9:3. ^{13}C NMR-DEPT-Hetcor (100.58 MHz, DMSO): some signals of 2 out of 3 rotamers are distinguishable δ = 18.3 ppm (p-CH_3), 22.0 ppm, 22.1 ppm and 22.2 ppm (3s, two belonging to the *anti* rotamer and the other to the *syn*, CH_3 of isoprop), 30.6 ppm (CH of isoprop), 41.2 ppm (d, $^1J_{PC}$ = 19 Hz, PCH_2N), 43.8 ppm (d, $^1J_{PC}$ = 19 Hz, PCH_2N), 46.9 ppm (d, $^1J_{PC}$ = 25 Hz, PCH_2N), 63.4–66.2 ppm (m, NCH_2N and $CO\underline{C}HCl_2$), 85.6, 86.0, 86.1 ppm (3s, CH arom), 88.8, 89.0, 89.4 ppm (3s, CH arom), 97.0 (s, C-quat, *anti*), 97.2 (s, C-quat, *syn*), 106.3 (s, C-quat), 162.1 ppm (s $\underline{C}OCHCl_2$, *syn*), 162.3 ppm and 162.5 ppm (2 s, $\underline{C}OCHCl_2$, *anti*). ^{1}H NMR (400 MHz, acetone-d_6): δ = 1.22 ppm (d, $^3J_{HH}$ = 6.8 Hz, 6H, CH_3 isop), below the solvent (p-CH_3), below the solvent (CH isoprop), 4.06 ppm (m, 3H of NCH_2P), 4.45 ppm (m, 2H, NCH_2P and NCH_2N), 4.88 ppm (m, 2H, NCH_2P and NCH_2N), 5.32 ppm (m, 2H, NCH_2P and NCH_2N), 5.62 ppm (d, 1H, $^2J_{HH}$ = 14.1 Hz, NCH_2N), 5.85 ppm (m, 4H, aromatic), 6.82 ppm and 6.90 ppm (2s, 2H, $CHCl_2$ of *anti* rotamers). ^{31}P NMR (acetone): δ = −8.1 ppm (s). Anal. Calcd. for $C_{19}H_{26}Cl_6N_3O_2PRu$: C 33.88, H 3.89, N 6.24; found C 33.86, H 3.74, N 5.95.

3.3.8. Synthesis and characterization of [Re(*o*-phen)(CO)$_3$DCP]NO_3 (8)

Solid $AgNO_3$ (19 mg, $1.14 \cdot 10^{-4}$ mol, MW 169.9 g/mol) was added to a solution of [ReCl(*o*-phen)$(CO)_3$] (50 mg, $1.09 \cdot 10^{-4}$ mol, MW 486.0 g/mol) in 5 mL of CH_3CN. The vial was placed in the microwave at 120 °C for 15 min. AgCl was eliminated by centrifugation and the ligand DCP (45 mg, $1.23 \cdot 10^{-4}$ mol, MW 367.0 g/mol 1.1 eq.) was added to the solution containing the solvento-complex [Re(*o*-phen)$(CO)_3(CH_3CN)$]NO_3. The mixture was placed again in the microwave at 120 °C for 15 min and a clear-yellow solution was obtained. The solution volume was reduced to a half and ether added (10 mL). The precipitate of [Re(*o*-phen)$(CO)_3$DCP]NO_3 was filtered and washed with ether (88 mg, $1.00 \cdot 10^{-4}$ mol, MW 879.4 g/mol, yield 92%). ^{1}H NMR (300 MHz, DMSO-d_6): δ = 3.6–5.6 ppm (m, DCP, 10H), 6.95 ppm (s, $CHCl_2$, *anti*) and 7.07 ppm (s, $CHCl_2$, *anti*), 7.10 ppm (s, $CHCl_2$, *syn*), 7.14 ppm (s, $CHCl_2$, *syn*), 8.18 ppm (m, $2H_c$, *o*-phen), 8.40 ppm (m, 2 H_d, *o*-phen), 9.1 ppm (m, 2 H_b, *o*-phen), 9.5 ppm (m, 2 H_a, *o*-phen). ^{31}P NMR (DMSO-d_6): δ = −57.8 ppm (s, *syn*), −47.9 ppm (s, *syn*), −42.3 ppm (s, *anti*, major). ^{1}H NMR/COSY (acetone-d_6, 400 MHz): three rotamers, δ = 4–5.6 ppm (m, DCP, 10H, 3 rotamers), 6.60 ppm and 6.72 ppm (2 s, $CHCl_2$, *anti*), 6.87 ppm, 7.21 and 7.38 ppm (s, $CHCl_2$, 2 *syn rotamers*), 8.23 ppm (dd, J_{HH} 8.6 Hz, J_{HH} 5.1 Hz) + 8.31 ppm (dd) + 8.35 (dd) ($2H_c$, *o*-phen), 8.38 ppm (s) + 8.48 ppm (s) + 8.50 (s) ($2H_d$, *o*-phen), 9.05 ppm (dd, J_{HH} 8.2 Hz, J_{HH} 1.6 Hz) + 9.15 ppm (m) ($2H_b$, *o*-phen), 9.58 ppm (dd J_{HH} 5.1 Hz, J_{HH} 1.6 Hz) + 9.62 ppm (dd) + 9.58 (d, J_{HH} 5.0 Hz) ($2H_a$, *o*-phen). ^{31}P NMR (acetone-d_6): δ = −58.3 ppm (s, *syn*), −52.1 ppm (s, *syn*), −41.7 ppm (s, *anti*, major). ^{13}C NMR (acetone-d_6): δ = 40–45 ppm (NCH_2P), 63–67 ppm (NCH_2N and $CHCl_2$), 127–157 ppm (*o*-phen), 162.7 ppm, 162.9 ppm, 163.1 ppm and 163.9 ppm (4s, $COCHCl_2$), 187.7 ppm (d, ReCO *trans* to P, $^2J_{PC}$ 64 Hz), 197.0 ppm (s, ReCO), 194.6 ppm (s, ReCO), 197.9 ppm (s, ReCO). ESI-MS: *m/z* 816 ($M^+ = C_{24}H_{20}Cl_4N_5O_5PRe$). UV–Vis (DMSO/PBS = 0.1 mL: 10 mL, 150 µM): λ_{max} = 275 nm (ε = 14,300 M^{-1} cm^{-1}), 370 nm (sh). Anal. Calcd. for $C_{24}H_{22}Cl_4N_6O_9PRe$: C 32.10, H 2.47, N 9.37; found C 31.92, H 2.39, N 9.13.

3.3.9. Synthesis and characterization of [AuCl(DCP)] (9)

The precursor [AuCl(tht)] (210 mg, $6.55 \cdot 10^{-4}$ mol, MW 320.6 g/mol) was dissolved in 30 mL of CH_2Cl_2. Solid DCP (240 mg, $6.55 \cdot 10^{-4}$ mol, MW 367.0 g/mol, 1 eq.) was added to the solution and the obtained suspension was left under stirring at room temperature for 2 h. The white precipitate was then filtered, washed with CH_2Cl_2 and dried under vacuum over P_2O_5 (335 mg, $5.59 \cdot 10^{-4}$ mol, MW 599.4 g/

mol, yield 85%).

^{1}H NMR (400 MHz, DMSO-d_6). *Anti* (major): 4.06 ppm (m, 3H), 4.32 ppm (d, $^{2}J_{HH}$ = 12.8 Hz, 1H), 4.46 ppm (d, $^{2}J_{HH}$ = 15.6 Hz,1H), 4.65 ppm (d, $^{2}J_{HH}$ = 14 Hz,1H), 4.97 ppm (m, 1H), 5.15 ppm (m, 2H), 5.47 ppm (d, $^{2}J_{HH}$ = 14 Hz,1H), 7.09 ppm (s, $CHCl_2$) and 7.18 ppm (s, $CHCl_2$); *syn-A* and *syn-B*: all the signals are overlapped to the *anti* signals except 7.20 ppm (s, $CHCl_2$), 7.25 ppm (s, $CHCl_2$). Estimated ratio: 12.8:1:1. ^{31}P NMR (121.44 MHz, DMSO): $\delta = -24.8$ ppm (s, *syn*), −19.3 ppm (s, *anti*, major), −18.4 ppm (s, *syn*) (ratio 1:12.5:1). ^{13}C NMR (100.58 MHz, DMSO-d_6). *Anti* (major): 44.0 ppm (d, $^{1}J_{PC}$ = 30.6 Hz, PCH_2N), 47.5 ppm (d, $^{1}J_{PC}$ = 29.2 Hz, PCH_2N), 63.3 ppm (d, $^{3}J_{PC}$ = 5.3 Hz, NCH_2N), 65.8 ppm (s, $CHCl_2$), 66.2 ppm (d, $^{3}J_{PC}$ = 5.3 Hz, NCH_2N), 66.4 ppm (s, $CHCl_2$), 162.4 ppm (s, CO), 162.7 ppm (s, CO). *syn-A* and *syn-B*: all the signals are overlapped to the *anti* signals except 65.3 ppm (s, $CHCl_2$), 65.6 ppm (s, $CHCl_2$).

^{31}P NMR (acetone-d_6): $\delta = -19.2$ ppm (s). Anal. Calcd. for $C_9H_{12}Cl_5N_3O_2PAu$:C 18.02, H 2.02, N 7.01; found C 17.91, H 1.86, N 6.96.

3.4. Single-crystal X-ray diffraction

Single-crystal diffraction data for DCP and complex **2** were collected at 295 K on a Nonius Kappa diffractometer equipped with a CCD detector with graphite-monochromated Mo Kα radiation (λ = 0.71069 Å). Intensities were corrected for Lorentz, polarization and absorption effects [62]. The structures were solved by direct methods with the SIR97 program and refinement were performed on F^2 by full matrix least-squares methods with all non-H atoms anisotropic. To model the disorder of DCP, the same crystallographic position has been assigned to P1 and N1 atoms, with a 50% occupancy [63].

In DCP, the hydrogen atoms were located in the difference-Fourier map and refined isotropically; in complex **2** the C-H hydrogens were included on calculated positions, riding on their carrier atoms, while it was impossible to locate the H atoms of the cocrystallized water molecule.

All calculations were performed using SHELXL2014/7 [64] implemented in the WinGX system of programs [65]. Experimental details are given in Table 8. A selection of bond distances and angles is reported in Tables 2, 4 and hydrogen bonding contacts parameters are reported in Tables 3 and 5. ORTEP-III [34] views of DCP and **2** are shown in Figs. 4 and 6, respectively.

CCDC 1859639-1859640 contain the supplementary crystallographic data for this paper. These data are provided free of charge by the Cambridge Crystallographic Data Centre.

3.5. Growth inhibition assays

The human ovarian cancer A2780 and A2780*cis* cell lines were obtained from ATCC (Manassas, VA) and maintained in RPMI 1640 medium (Lonza, Verviers, Belgium), supplemented with 10% fetal bovine serum (FBS; Biowest, Nuaillé, France), 50 units/mL penicillin (Lonza, Verviers, Belgium) and 50 µg/mL streptomycin (Lonza, Verviers, Belgium). To conserve the resistance, 1 µM cisplatin was routinely added to the A2780*cis* cells. The pH of the medium was 7.2 and the incubation was performed at 37 °C in a 5% CO_2 humidified atmosphere. The A2780 and A2780*cis* cells were detached from the tissue culture flasks as follows: after a gentle cleanup with 1X PBS, trypsin (100 µL/well) was added. After 3 min incubation at 37 °C, FBS (100 µL/well) and RPMI (800 µL/well) are added.

The human erythroleukemia K562 cells were isolated and characterized by Lozzio CB and Lozzio BB, from a patient with chronic myelogenous leukemia (CML) in blast crisis [66]. K562 cells were cultured in humidified atmosphere of 5% CO_2, in RPMI-1640 medium (Lonza, Verviers, Belgium) supplemented with 10% fetal bovine serum (FBS; Biowest, Nuaillé, France), 50 units/mL penicillin (Lonza, Verviers, Belgium) and 50 µg/mL streptomycin (Lonza, Verviers, Belgium) [67].

Table 8
Experimental details.

	DCP	Complex **2**
Chemical formula	$C_9H_{12}Cl_4N_3O_2P$	$C_{18}H_{24}Cl_{10}N_6O_4P_2Pt{\cdot}H_2O$
M_r	366.99	1017.98
Crystal system, space group	Monoclinic, *C*2/*c*	Triclinic, $P\bar{1}$
a, *b*, *c* (Å)	15.4455 (8), 9.6375 (6), 10.2555 (4)	9.7176(3), 13.3124(4), 14.5640(4)
α, β, γ (°)	90, 105.066 (3), 90	116.055(2), 94.649(2), 90.310(2)
V (Å^3)	1474.12 (13)	1685.25 (9)
Z	4	2
µ (mm^{-1})	0.91	5.09
Crystal size (mm)	0.48 × 0.24 × 0.19	0.15 × 0.10 × 0.06
No. of measured, independent and observed [$I > 2s(I)$] reflections	6589, 1750, 1492	28,836, 7350, 6563
R_{int}	0.028	0.062
$R[F^2 > 2s(F^2)]$, $wR(F^2)$, S	0.074, 0.206, 1.09	0.036, 0.093, 1.06
No. of reflections/ parameters	1750/121	7350/380
$\Delta\rho_{max}$, $\Delta\rho_{min}$ (e Å^{-3})	0.87, −0.83	1.60, −1.65

The derivatives were added to cell cultures at serial dilutions and incubated for 72 h. For the stock mother solution, the compounds have been dissolved in DMSO at the final concentration of 50 mM. All the working solutions of the complexes were obtained following a further dilution using pure DMSO, in order to obtain 50 µM concentrations. Finally the compounds were diluted in the complete medium (RPMI and FBS) in order to obtain the final concentrations to be used on the cells (the DMSO concentration never exceeded 0.2% concentration). In any case control experiments demonstrated lack of biological effects of the DMSO vehicle. Cisplatin (diluted in H_2O) was employed as control for all the cell lines, A2780, A2780*cis* and K562. Untreated cells were placed in every plate as negative control. The vehicle DMSO was verified to be not able to induce antiproliferative activity. The cells were exposed to the compounds in 1000 µL total volume. Cells were finally suspended in physiological solution and counted with a Z2 Coulter Counter (Coulter Electronics, Hialeah, FL, USA). The cell number/mL was determined as IC_{50} after 3 days of culture, when untreated cells are in log phase of growth [52–54].

3.6. Apoptosis assays

Annexin V and Dead Cell assays on A2780, A2780*cis* and K562 cells, untreated and treated for 72 h with different doses of analyzed derivatives, were performed with a Muse™ Cell Analyzer (Millipore, Billerica, MA, USA), according to the instructions supplied by the manufacturer [52,68–69]. This procedure is based on Annexin V to detect PS (PhosphatidylSerine) on the external membrane of apoptotic cells. Moreover, a dead cell marker was employed in the same kit as indicator of cell membrane structural integrity. Cells were diluted (1:1) with the one step addition of the Muse Annexin V & Dead Cell reagent. After 20 min of incubation between cell samples and kit at room temperature in the dark, samples were analyzed. Data were acquired and recorded utilizing the Annexin V and Dead Cell Software Module (Millipore, Billerica, MA, USA).

3.7. Cell differentiation evaluation

Erythroid differentiation was assayed on K562 cells treated with all the complexes in comparison with the known inducer cisplatin [58]. Cells were cultured for 7 days and the enzymatic-colorimetric benzidine

test was used to determine the possible effects after 5, 6 and 7 days culture of K562 cells incubated with different concentrations of derivatives.

4. Conclusions

The new ligand DCP, designed as a carrier of either proapoptotic dichloroacetic acid and a cytotoxic metal ion, was obtained in high yield under appropriate conditions (pH, solvent and reagents ratio). Its structural features, including the presence of rotameric forms due to the hindered rotation around the amidic CN bonds, were studied both in solution (NMR and ESI-MS) and in solid (X-ray crystal structure). The coordination of DCP acting as a P-donor to a variety of cytotoxic metal ions, (Pt^{2+}, Pd^{2+}, Ru^{2+}, Re^{+}, Au^{+}) gave nine new complexes, whose antiproliferative and proapoaptotic activity in human tumor cell lines have been tested.

The antiproliferative activity was tested in vitro on cisplatin-sensitive A2780, cisplatin-resistant A2780*cis* and K562 cell lines, in comparison with cisplatin, used as positive standard.

Platinum complexes **3** for A2780 cells, **2**, **3** and **4** for A2780*cis* cells and **4** for K562, displayed antiproliferative comparable to cisplatin and higher than the free ligand DCP showing that the simultaneous presence of DCP (containing two residues of proapoptotic DCA) and Pt(II) produces the best performances.

Moreover, it was observed that the anti-proliferative activity of the most active Pt(II) complexes is associated with induction of apoptosis.

On the contrary, the association of DCP with other active metal ions did not give good results, with the exception of the complexes containing Pd (**5** and **6**), Ru (**7**) and Au (**9**), that showed a remarkable proapoptotic activity on the erythroleukemic K562 cell line.

Although more specific tests are necessary for clarifying the target of the compounds here presented, the apoptosis mechanisms seem to be involved.

Abbreviations

DCP	3,7-bis(dichloroacetyl)-1,3,7-triaza-5-phosphabicyclo[3.3.1]nonane
DCA	dichloroacetic acid/dichloroacetate
PTA	1,3,5-triaza-7-phosphaadamantane

Funding

This work was supported by University of Ferrara (Grant FAR 2017 to IL) and CIRCMSB (Consorzio Interuniversitario di ricerca in chimica dei metalli nei sistemi biologici). R.G. is funded by AIRC (Associazione Italiana Ricerca sul Cancro) and by CIB (Consorzio Interuniversitario per le Biotecnologie).

Declaration of Competing Interest

No potential conflicts of interest were disclosed.

Acknowledgements

We thank E. Bianchini, P. Formaglio, T. Bernardi and D. Preti for technical assistance.

Appendix A. Supplementary data

Supplementary data to this article can be found online at https://doi.org/10.1016/j.jinorgbio.2019.110787.

References

[1] P. Barbaro, L. Gonsalvi, A. Guerriero, F. Liguori, Green Chem. 11 (2012) 3211–3219.
[2] S. Moret, P.J. Dyson, G. Laurenczy, Nature Comm 5 (2014) 4017–4023.
[3] M.A. Affan, P.G. Jessop, Inorg. Chem. 56 (2017) 7301–7305.
[4] F. Scalambra, N. Holzmann, L. Bernasconi, S. Imberti, A. Romerosa, ACS Catal. 8 (2018) 3812–3819.
[5] M. Serrano-Ruiz, P. Lorenzo-Luis, A. Romerosa, A. Mena-Cruz, Dalton Trans. 42 (2013) 7622–7630.
[6] S.W. Jaros, M.F.C. Guedes da Silva, J. Krol, M. Conceicao Oliveira, P. Smolenski, A.J.L. Pombeiro, A.M. Kirillov, Inorg. Chem. 55 (2016) 1486–1496.
[7] S.W. Jaros, M.F.C. Guedes da Silva, M. Florek, P. Smolenski, A.J.L. Pombeiro, A.M. Kirillov, Inorg. Chem. 55 (2016) 5886–5894.
[8] B. Sierra-Martin, M. Serrano-Ruiz, V. Garcia-Sakai, F. Scalambra, A. Romerosa and A. Fernandez-Barbero, Polymers 10 (2018) 528/1–528/12.
[9] F. Battistin, F. Scaletti, G. Balducci, S. Pillozzi, A. Arcangeli, L. Messori, E. Alessio, J. Inorg. Biochem. 160 (2016) 180–188.
[10] R. Pettinari, A. Petrini, F. Marchetti, C. Pettinari, T. Riedel, B. Therrien, P.J. Dyson, Eur. J. Inorg. Chem. (12) (2017) 1800–1806.
[11] R.H. Berndsen, A. Weiss, U.K. Abdul, T.J. Wong, P. Meraldi, A.W. Griffioen, P.J. Dyson, P. Nowak-Sliwinska, Sci. Rep. 7 (2017) 43005.
[12] B.S. Murray, M.V. Babak, C.G. Hartinger, P.J. Dyson, Coord. Chem. Rev. 306 (2016) 86–114.
[13] P. Bergamini, L. Marvelli, A. Marchi, F. Vassanelli, M. Fogagnolo, P. Formaglio, T. Bernardi, R. Gavioli, F. Sforza, Inorg. Chim. Acta 391 (2012) 162–170.
[14] R. Cortesi, P. Bergamini, L. Ravani, M.S. Drechsler, A. Costenaro, M. Pinotti, M. Campioni, L. Marvelli, E. Esposito, Int. J. Pharm. 431 (2012) 176–182.
[15] P. Bergamini, L. Marvelli, A. Marchi, V. Bertolasi, M. Fogagnolo, P. Formaglio, F. Sforza, Inorg. Chim. Acta 398 (2013) 11–18.
[16] V. Ferretti, M. Fogagnolo, A. Marchi, L. Marvelli, F. Sforza, P. Bergamini, Inorg. Chem. 53 (2014) 4881–4890.
[17] R. Cortesi, C. Damiani, L. Ravani, L. Marvelli, E. Esposito, M. Drechsler, A. Pagnoni, P. Mariani, F. Sforza, P. Bergamini, Int. J. Pharm. 492 (2015) 291–300.
[18] J.M. Forward, Z. Assefa, R.J. Staples, J.P. Fackler Jr., Inorg. Chem. 35 (1996) 16–22.
[19] A.M. Kirillov, P. Smolenski, M. Haukka, M.F.C. Guedes da Silva, A.J.L. Pombeiro, Organometallics 28 (2009) 1683–1687.
[20] E. Atrian-Blasco, S. Gascon, M.J. Rodriguez-Yoldi, M. Laguna, E. Cerrada, Eur. J. Inorg. Chem. (17) (2016) 2791–2803.
[21] A. Guerriero, M. Peruzzini, L. Gonsalvi, Coord. Chem. Rev. 355 (2018) 328–361.
[22] D.J. Darensbourg, C.G. Ortiz, J.W. Kamplain, Organometallics 23 (2004) 1747–1754.
[23] D.A. Krogstad, G.S. Ellis, A.K. Gunderson, A.J. Hammrich, J.W. Rudolf, J.A. Halfen, Polyhedron 26 (2007) 4093–4100.
[24] W. Liu, J. Jiang, Y. Xu, S. Hou, L. Sun, Q. Ye, L. Lou, J. Inorg. Biochem. 146 (2015) 14–18.
[25] X.X. Stander, B.A. Stander, A.M. Joubert, Cell. Physiol. Biochem. 35 (2015) 1499–1526.
[26] E. Babu, S. Ramachandran, V. Coothankandaswamy, S. Elangovan, P.D. Prasad, V. Ganapathy, M. Thangaraju, Oncogene 30 (2011) 4026–4037.
[27] R.K. Pathak, S. Marrache, D.A. Harn, S. Dhar, ACS Chem. Biol. 9 (2014) 1178–1187.
[28] C. Trapella, R. Voltan, E. Melloni, V. Tisato, C. Celeghini, S. Bianco, A. Fantinati, S. Salvadori, R. Guerrini, P. Secchiero, G. Zauli, J. Med. Chem. 59 (2016) 147–156.
[29] D.J. Darensbourg, J.B. Robertson, D.L. Larkins, J.H. Reibenspies, Inorg. Chem. 38 (1999) 2473–2481.
[30] E. Bisz, A. Piontek, B. Dziuk, R. Szostak, M. Szostak, J. Org. Chem. 83 (2018) 3159–3163.
[31] E. Vergara, S. Miranda, F. Mohr, E. Cerrada, E.R.T. Tiekink, P. Romero, A. Mendía, M. Laguna, Eur. J. Inorg. Chem. (2007) 2926–2933.
[32] K. Sungsoo, K. Jungyu, K. Jieun, W. Daeun, C. Suk-Kyu, C. Wansik, J. Keunhong, A. Sangdoo, K. Kyungwon, Molecule 23 (2018) 2294–2312.
[33] V. Prelog, G. Helmchen, Angew. Chemie 21 (1982) 567–583.
[34] M.N. Burnett, C.K. Johnson, ORTEP-III: oak ridge thermal ellipsoid plot program for crystal structure illustrations, Oak Ridge National Laboratory Report ORNL-6895, 1996.
[35] G. Cavallo, P. Metrangolo, R. Milani, T. Pilati, A. Primagi, G. Resnati, G. Terraneo, Chem. Rev. 116 (2016) 2478–2601.
[36] A.R. Kapdi, I.J.S. Fairlamb, Chem. Soc. Rev. 43 (2014) 4751–4777.
[37] E. Guerrero, S. Miranda, S. Lüttenberg, N. Fröhlich, J.-M. Koenen, F. Mohr, E. Cerrada, M. Laguna, A. Mendía, Inorg. Chem. 52 (2013) 6635–6647.
[38] M. Carreira, R. Calvo-Sanjuán, M. Sanaú, I. Marzo, M. Contel, Organometallics 31 (2012) 5772–5781.
[39] C.S. Allardyce, P.J. Dyson, D.J. Ellis, S.L. Heath, Chem. Comm. (2001) 1396–1397.
[40] C.S. Allardyce, A. Dorcier, C. Scolaro, P.J. Dyson, Appl. Organomet. Chem. 19 (2005) 1–10.
[41] A. Dorcier, P.J. Dyson, C. Gossens, U. Rothlisberger, R. Scopelliti, I. Tavernelli, Organometallics 24 (2005) 2114–2123.
[42] R. Pettinari, F. Condello, F. Marchetti, C. Pettinari, P. Smoleński, T. Riedel, R. Scopelliti, P.J. Dyson, Eur. J. Inorg. Chem. (22) (2017) 2905–2910.
[43] C. Scolaro, A. Bergamo, L. Brescacin, R. Delfino, M. Cocchietto, G. Laurenczy, T.J. Geldbach, G. Sava, P.J. Dyson, J. Med. Chem. 48 (2005) 4161–4171.
[44] P. Nowak-Sliwinska, J.R. van Beijnum, A. Casini, A.A. Nazarov, G. Wagnières, H. van den Bergh, P.J. Dyson, A.W. Griffioen, J. Med. Chem. 54 (2011) 3895–3902.
[45] S.C. Marker, S.N. MacMillan, W.R. Zipfel, Z. Li, P.C. Ford, J. Wilson, Inorg. Chem. 57 (2018) 1311–1331.
[46] P. Kurz, B. Probst, B. Spingler, R. Alberto, Eur. J. Inorg. Chem. (2006) 2966–2974.
[47] I. Ott, Coord. Chem. Rev. 253 (2009) 1670–1681.
[48] S. Jurgens, A. Casini, Chimia 71 (2017) 92–101.

[49] O. Karaca, V. Scalcon, S.M. Meier-Menches, R. Bonsignore, J.M.J.L. Brouwer, F. Tonolo, A. Folda, M.P. Rigobello, F.E. Kuehn, A. Casini, Inorg. Chem. 56 (2017) 14237–14250.
[50] B. Bertrand, A. Citta, I.L. Franken, M. Picquet, A. Folda, V. Scalcon, M.P. Rigobello, P. Le Gendre, A. Casini, E. Bodio, J. Biol. Inorg. Chem. 20 (2015) 1005–1020.
[51] Z. Assefa, B.G. McBurnett, R.J. Staples, J.P. Fackler Jr., B. Assmann, K. Angermaier, H. Schmidbaur, Inorg. Chem. 34 (1995) 75–83.
[52] T. Scattolin, I. Caligiuri, L. Canovese, N. Demitri, R. Gambari, I. Lampronti, F. Rizzolio, C. Santo, F. Visentin, Dalton Trans. 47 (2018) 13616–13630.
[53] T. Scattolin, L. Canovese, F. Visentin, S. Paganelli, P. Canton, N. Demitri, Appl. Organomet. Chem. 32 (2018) e4034.
[54] P. Bergamini, L. Marvelli, V. Ferretti, C. Gemmo, R. Gambari, Y. Hushcha, I. Lampronti, Dalton Trans. 45 (2016) 10752–10760.
[55] K.M. Henkels, J.J. Turchi, Cancer Res. 59 (1999) 3077–3083.
[56] S. Dasari, P.B. Tchounwou, Eur. J. Pharmacol. 740 (2014) 364–378.
[57] V. Ferretti, P. Bergamini, L. Marvelli, Y. Hushcha, C. Gemmo, R. Gambari, I. Lampronti, Inorg. Chim. Acta 470 (2018) 119–127.
[58] I. Lampronti, N. Bianchi, C. Zuccato, A. Medici, P. Bergamini, R. Gambari, Bioorg. Med. Chem. 14 (2006) 5204–5210.
[59] D.J. Daigle, Inorg. Synth. 32 (1998) 40–45.
[60] S. Otto, A. Roodt, W. Purcell, Inorg. Chem. Commun. 1 (1998) 415–417.
[61] R. Usón, A. Laguna, M. Laguna, Inorg. Synth. 26 (1989) 85–91.
[62] R.H. Blessing, Acta Crystallogr. A 51 (1995) 33–38.
[63] A. Altomare, M.C. Burla, M. Camalli, G. Cascarano, C. Giacovazzo, A. Guagliardi, A.G. Moliterni, G. Polidori, R. Spagna, J. Appl. Crystallogr. 32 (1999) 115–119.
[64] G.M. Sheldrick, Acta Crystallogr. C 71 (2015) 3–8.
[65] L.J. Farrugia, J. Appl. Crystallogr. 45 (2012) 849–854.
[66] C.B. Lozzio, B.B. Lozzio, Blood 45 (1975) 321–334.
[67] I. Lampronti, M.T. Khan, M. Borgatti, N. Bianchi, R. Gambari, eCAM. 5 (2008) 303–312.
[68] A. Baldisserotto, S. Vertuani, A. Bino, D. De Lucia, I. Lampronti, R. Milani, R. Gambari, S. Manfredini, Bioorg. Med. Chem. 23 (2015) 264–271.
[69] R. Milani, E. Brognara, E. Fabbri, A. Finotti, M. Borgatti, I. Lampronti, G. Marzaro, A. Chilin, K.K. Lee, S.H. Kok, C.H. Chui, R. Gambari, Oncol. Res. 26 (2018) 1307–1315.